Jurnal Teknologi

Full Paper

DESIGN AND FABRICATION OF FIV APPARATUS FOR CLASSROOM LECTURE DEMONSTRATION

Masataka Shirakashi, Chih Ping Chua, Sheikh Ahmad Zaki*

Malaysian-Japan International Institute of Technology, Universiti Teknologi Malaysia, Malaysia

Article history
Received
9 July 2015
Received in revised form
17 March 2016
Accepted
15 August 2016

*Corresponding author
sheikh.kl@utm.my

Graphical abstract

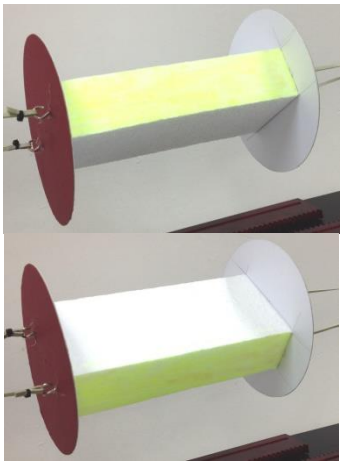

Abstract

Flow induced vibrations (FIVs) of a cylinder commonly occur where a cylindrical body is exposed to a flow. However, their appearance and behavior are widely diverging depending on flow condition and characteristics of cylinder with its supporting structure, making their prediction quite difficult. Hence, many serious accidents have been caused so far for structures and machines. Most typical and well-known FIVs in this category are the Karman vortex induced vibration (KVIV), the galloping and the torsional flutter. In this work, a very simple and convenient apparatus is designed and made to reproduce these three vibrations. This apparatus will be effective in a classroom lecture of fluid mechanics by demonstrating how easily the FIVs can be induced by a simple apparatus, even though their prediction remains to be important but difficult problems to be solved in practical engineering.

Keywords: Flow induced vibration, Karman vortex, Galloping, Torsional flutter, Fluid mechanics education

Abstrak

Getaran yang berpunca daripada pengaliran bendalir biasanya berlaku apabila badan silinder terdedah kepada pengaliran bendalir. Walau bagaimanapun, penampilan dan pergerakan getaran tersebut bergantung kepada keadaan aliran dan ciri-ciri silinder dengan struktur penyokongnya. Ini menyebabkan keadaan getaran in sukar diramal. Oleh itu, banyak kemalangan yang disebabkan oleh getaran berpunca daripada pengaliran bendalir kerap berlaku sehingga kini. Fenomena-fenomena getaran berpunca daripada pengaliran bendalir yang biasa dikenali adalah getaran disebabkan vorteks Karman (KVIV), getaran mencongklang dan getaran kilasan. Dalam projek ini, alat yang boleh menghasilkan ketiga-tiga getaran tersebut telah direka dan difabrikasi. Alat yang difabrikasi ini akan membantu dalam pengajaran mekanik bendalir dan lebih senang difahami oleh pelajar dengan menunjukkan ketiga-tiga getaran yang biasa dikenali di dalam kuliah, walaupun ramalan terhadap pembentukan getaran berpunca daripada pengaliran bendalir masih merupakan masalah penting yang perlu diselesaikan.

Kata Kunci: Getaran yang berpunca daripada pengaliran bendalir, vortex Karman, Getaran mencongklang, Getaran kilasan, Pendidikan mekanik bendalir

1.0 INTRODUCTION

Flow induced vibrations (FIVs) are very commonly observed where flexible or spring supported body is contacting with fluid flow [1]. Among them, vibration of a cylindrical body immersed in a flow is of practical importance since such circumstance is prevailing in civil and mechanical engineering applications. Since the behaviors and mechanisms of FIVs in this category is widely diverging depending on the flow conditions and characteristics of the cylinder including its support, there exists no general way to predict and avoid them. Hence, many accidents have been caused by this category of FIVs, e.g. the collapse of Tacoma Narrows Bridge shown in Figure 1. This accident was triggered by Karman vortex induced vibration (KVIV), which transited to the torsional flutter leading to the collapse of the bridge. In addition to these two, another type of cylinder vibration called galloping is known to occur at velocities higher than that of KVIV [2], [3], [4], [5], [6], [7], [8], [9], [10].

Although basic understandings of the mechanisms of these FIVs have been obtained, there exists no theoretical way to predict their occurrence and behaviors against varying velocity due to the fact that the difficulty in solving the equation of fluid motion (Navier–Stokes (N-S) equation) is unsurmountable. In addition, the essential difficulty becomes even larger due to the feedback effect of vibration which constitutes the boundary condition of N-S equation to the exciting fluid force as seen in Figure 2. In addition, another difficulty from the practical point of view comes from the fact that slight change of conditions can largely affect the vibration behavior. Therefore, to cope with practical problems, semi-empirical equation systems called an oscillator model are introduced to relate the exciting force to the vibration behavior based on the model experiments, as shown in Figure [1], [2], [4], [8], [11].

To obtain the understanding on mechanisms of the FIVs, the flow/vibrating-cylinder system is usually simplified as follows.

1) The cylinder is rigid (no deformation).
2) The cylinder is supported by spring so as to allow translational motion in crossflow direction, or rotation around its axis (one-degree-of-freedom vibration).
3) The vibrating system is linear, i.e. specified by mass *m*, damping factor *c* and spring constant *k*.
4) The flow approaching the cylinder is steady and uniform, resulting in two dimensional flows around the vibrating cylinder.

By applying these assumptions, the system for the case of crossflow vibration is modelled as shown in Figure 3.

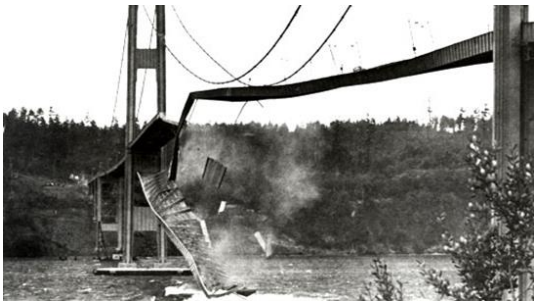

Figure 1 Collapse of Tacoma Narrows Bridge, 1940, USA [14]

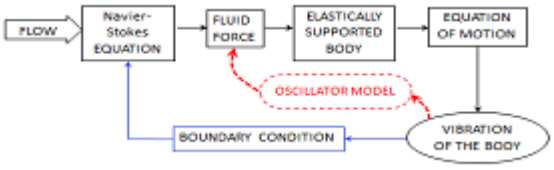

Figure 2 Structure of FIV problem

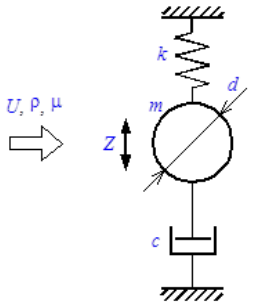

Figure 3 Simplified model of a cylinder exposed to flow for crossflow vibration

In spite of the simplicity of the model, it shows the three types of FIVs, which still remain to be unsolved problems in fluid science and engineering. The specific aim of this study is to design and fabricate an apparatus for the simplified model to reproduce the three FIVs in order to use in classroom lectures for high school or undergraduate course of university. This apparatus will be effective in fluid mechanics education by demonstrating in a classroom lecture how easily the FIVs can be induced by a simple apparatus on one hand, and how difficult to predict the vibration behavior on the other hand.

2.0 ANALYTICAL APPROACH AND DIFFICULTIES

2.1 Equation of Cylinder Motion

Let the crossflow displacement of the cylinder Z, then the equation of motion for the cylinder in Figure 3 is written as

$$m\frac{d^2Z}{dt^2} + c\frac{dZ}{dt} + kZ = F_z(t) \quad (1)$$

Here, *Fz* on the right hand side is the z-direction force exerted on the cylinder by the fluid, which is determined by the fluid motion around the cylinder. The buoyancy force is usually neglected by measuring Z from the equilibrium position.

The difficulty of FIV problem comes from the fact that it is generally impossible to solve N-S equation, especially when the cylinder is vibrating. In addition, the cylinder motion caused by *Fz* changes the boundary condition of N-S equation, thus giving a feedback effect to *Fz* as seen in Figure 2. Hence, for practical engineering purposes, empirical expressions for *Fz* as a function of *Z* and its derivatives are proposed depending on each circumstance, as indicated by OSCILLATOR MODEL in Figure 2.

One common way to simplify the problem is to divide *Fz* into two contributions, the resistance force which exists even when the flow velocity *U*=0 and fluid force generated by the flow, i.e. the lift F_L. The former is usually assumed to be composed of an inertial and a frictional component to give the following expression.

$$F_z = -m_{add}\frac{d^2Z}{dt^2} - c_{add}\frac{dZ}{dt} + F_L \quad (2)$$

Here, m_{add} and c_{add} are called additional mass and additional damping factor, respectively. The assumption leading to Equation (2) is not correct since the drag force is nearly proportional with the square of the cylinder velocity *dZ/dt* for wide range of conditions such as the geometry of the body and Reynolds number *Re*. Nevertheless, m_{add} and c_{add} in Equation (2) are regarded to be constant in most of analytical approach since it can give considerably satisfying approximation.

Thus, introducing the effective mass and the effective damping defined by

$$m_e = m + m_{add} \quad (3a)$$

$$c_e = c + c_{add} \quad (3b)$$

Equation (1) is rewritten as

$$m_e\frac{d^2Z}{dt^2} + c_e\frac{dZ}{dt} + kZ = F_L(t) \quad (4)$$

In this equation, F_L=0 when *U*=0. Hence, if we may take m_e and c_e constant, the solution of Equation (4) for the free-damping oscillation in fluid otherwise at rest with initial conditions

$$Z=Zo \text{ and } dZ/dt=0 \text{ at } t=0 \quad (5)$$

is written as

$$Z = Z_0 e^{-\zeta\omega_n t}\cos\omega_n t \quad (6)$$

when the damping ratio $\zeta = c/c_c \ll 1$. Here, $\omega_n = \sqrt{k/m_e}$ is the natural angular frequency and $c_c = 2\sqrt{m_e k}$ is the critical damping factor.

2.2 Analysis of Vortex-Induced Vibrations (VIVs)

In VIVs, the frequency of exciting force is equal to the vortex shedding frequency *fv*, and then the vibration frequency *fz=fv*. Then, we can assume that

$$Z = Z_A \sin(2\pi f_v t) \quad (7)$$

and

$$F_L = F_{LA}\sin(2\pi f_v t + \phi) \quad (8)$$

Then, equation (4) gives

$$Z_A = \frac{F_{LA}}{k}\frac{1}{\sqrt{\left(1 - {f_v}^{*2}\right)^2 + (2\zeta {f_v}^*)^2}} \quad (9)$$

and

$$\tan\phi = \frac{2\zeta {f_v}^*}{1 - {f_v}^{*2}} \quad (10)$$

where $f_n = \omega_n/2\pi$ is the natural frequency and $f_v^* = f_v/f_n$ is non-dimensional vortex shedding frequency.

If the amplitude F_{LA} and frequency *fv* of the exciting force were given as the external force which are independent of the vibration, the vibration amplitude given by Equation (9) would be maximum when the exciting force frequency *fv* was equal to the natural frequency of the cylinder *fn*. By introducing non-dimensionalized variables, the maximum amplitude would be written as

$$Z_{A\,max}^* = \frac{Z_{A\,max}}{d} = \frac{1}{\pi^2}\cdot\frac{C_L {U_R}^{*2}}{Sc} \quad (11)$$

Here, $S_C = 2M_R\delta$ is Scruton number, M_R is the mass ratio (= mass of the cylinder / mass of displaced fluid), $U_R^* = U_R/f_n d$ is the reduced velocity at the resonance, and C_L the lift coefficient defined by $F_{LA} = 0.5C_L\rho U^2 dL$ (*L* = cylinder length). Equation (11) shows that $Z_{A\,max}^* S_C$ will give a fair comparison for maximum amplitude of VIVs with geometrically similar but with different structure parameter systems.

The most remarkable difference of VIV from the usual resonance is that the vibration can change the exciting force causing the vibration itself. The most prominent feedback effect appears as so-called "synchronization (or lock-in)" of vortex shedding to the cylinder vibration, in which the vortex shedding is controlled by, or attracted to, the cylinder vibration, making *fv=fz* even when the natural vortex shedding frequency f_{v0} (*fv* for the cylinder at rest) is considerably deviating from *fz*. The velocity range

with large vibration amplitude is considerably widened by the synchronization. Besides, the magnitude of exiting force F_{LA} is reported to become larger by the synchronization.

At the present stage, analytical approach is not successful since:

1) The condition for synchronization is not clear.
2) F_{LA} and Φ under synchronization are unknown.
3) When the vortex shedding is synchronizing with the cylinder oscillation, the flow field around the cylinder is determined by the vortex shedding.

Therefore, the additional mass and the additional damping should be regarded as vanishing. However, Equation (4) is still used since there exists no better alternative way.

Recently, T. Nguyen *et al*. explained why the behaviors of VIVs are deviating from usual resonance and proposed a new oscillator model [11] applicable to VIVs in general.

2.3 Galloping and Torsional Flutter

When the cross section of the cylinder is square, or rectangular in general, it is known that another crossflow vibration called galloping occurs at velocities considerably higher than that of KVIV. The amplitude of galloping increases divergently with the flow velocity while that of KVIV is limited in a certain velocity range around $U=U_0$ (U_0 is the velocity at which $fv_0= fn$), as seen later in Figure 10 (b).

The mechanism of galloping is explained as follows. When the cylinder moves in positive Z direction, the flow relative to the cylinder U_r will have a relative attack angle α_r, making the time-averaged flow field non-symmetric between upper and lower sides of the cylinder. If the fluid force generated by this non-symmetric flow is acting to the equal direction of the initial cylinder motion, i.e. positive Z direction, the system is unstable and can result in a vibration. This is equivalent to say that the fluid force has negative damping effect. In this discussion, the alternating force of vortex shedding has much shorter period than the cylinder motion so that it is smoothed out during a cycle of vibration.

In the case of torsional flutter, Equation (4) is rewritten for the rotational motion of the cylinder. The mechanism of torsional flutter is similar to the galloping in the sense that instability against an initial angular displacement of the cylinder causes the vibration. Hence these two are classified as the Fluid-elastic instability vibration (FEV). While the galloping is attributed to the negative damping effect of the fluid force, the torsional flutter is caused by both the negative damping and the negative spring effects of the fluid force moment.

Since the lift force of a circular cylinder is zero at an arbitrary attack angle, the galloping and the torsional flutters are not observed for a circular cylinder.

3.0 STRUCTURE OF APPARATUS

Figure 4 shows the structure of wind tunnel made in this study. A commercial fan (Andover TYPE 630-J) adjustable at three velocities is used to generate air flow. The wind collecting chamber, the contraction chamber and the nozzle are made of color card board. In the nozzle, bundle of plastic straws with 12 mm diameter×180mm length is set as the flow straightener.

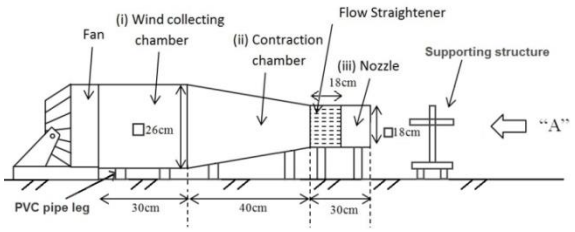

Figure 4 Structure of wind tunnel using a commercial fan

A circular, a square and a rectangular cylinder were made as the test cylindrical body. Table 1 gives the dimension of three cylinders used in this study. Styrofoam is selected as the material since it has low density and is easy to be processed. Circular plates with a diameter 120 mm made of the same card board used for the wind tunnel are attached to both ends of cylinders to reduce the end effect and thus to make the flow two dimensional over the whole span of the cylinder. The dimension and mass of the cylinders are given in Table 1. The cylinder is set horizontally at the exit of the wind tunnel nozzle supported by tensioned rubber strings as shown in Figure 5.

Table 1 Dimensions and mass of cylinders

Cylindrical body	Overview	Dimension, cm	Mass, g
Circular	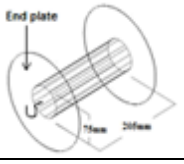	Diameter, d = 7.5 Span length, L = 20.5	39.65
Square	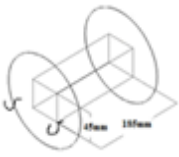	Side length, d = 4.5 Span length, L = 18.5	31.05
Rectangular	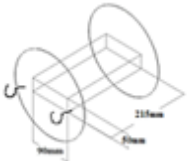	Streamwise side, B = 9.0 Height, d = 5.0 Span length, L = 21.5	58.12

The length of the rubber strings is adjusted by a rack-pinion mechanism in order to change the initial tensile force. The effective spring constant for the vertical motion is controlled by adjusting the initial tensile force, while that for the torsional motion is adjusted by the separation of the two strings at each end. Thus the spring constants for the two motions can be selected independently by adjusting the tensile force and distance of the two rubber strings at each end of the cylinder.

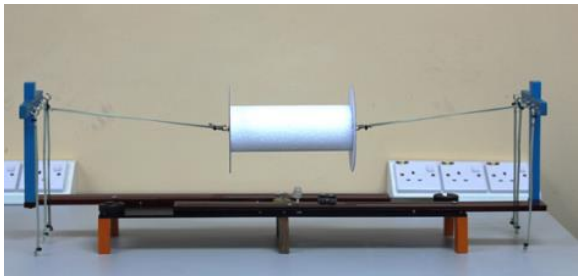

Figure 5 Supporting structure viewed from "A" in Figure 4

4.0 EXPERIMENTAL RESULTS

4.1 Characteristics of Flow at the Nozzle Exit

The wind velocity distribution at the nozzle exit was measured by wind velocity meter (EXTECH INSTRUMENTS 45160) at points shown in Figure 6. Velocity distribution thus obtained is given in Figure 7. The contraction chamber and the nozzle installed with the flow straightener make the velocity profile uniform although the original flow of the fan has whirling component with dented profile in the region around the axis. However, the velocity is reduced because of the contraction and resistance of the flow straightener in the nozzle.

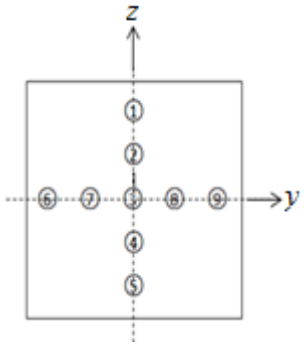

Figure 6 Points of wind velocity measurement viewed from "A" in Figure 4

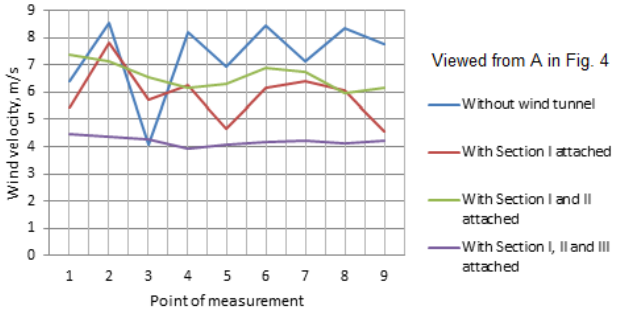

Figure 7 Velocity distribution of wind tunnel at maximum speed position of the fan

4.2 Determination of Structural Parameters

Images of cylinder motion are recorded by a digital camera, together with a scale to measure the displacement Z. From the reproduced images, the oscillogram of Z is determined by curve fitting.

Figure 8 shows an example of free damping oscillation, i.e. the displacement Z at $U = 0$ with initial conditions $Z = Zo > 0$ and $dZ/dt = 0$. From this figure, the natural frequency f_n is obtained by counting the number of cycles in a certain time, and the logarithmic damping factor δ is determined by:

$$\delta = \frac{1}{m} \ln \frac{Z_n}{Z_{n+m}} \tag{12}$$

The effective mass m_e, damping ratio ζ, the critical damping factor c_c and the effective damping factor c_e are determined by the following equations derived from Equation (6).

$$m_e = \frac{k}{\omega_n^2} \tag{13}$$

$$c_c = 2\sqrt{m_e k} \tag{14}$$

$$\zeta = \frac{\delta}{2\pi} \tag{15}$$

$$c_e = \zeta \, c_c \tag{16}$$

Here, the spring constant k is determined by calibration experiment performed by putting weight on the cylinder and measuring the vertical displacement Z as shown in Figure 9.

Table 2 gives the values of the above structural parameters for the circular and square cylinders for the vibration experiment to be explained in Section 4.3. The effective mass m_e is considerably larger than those expected from the inviscid fluid theory [1].

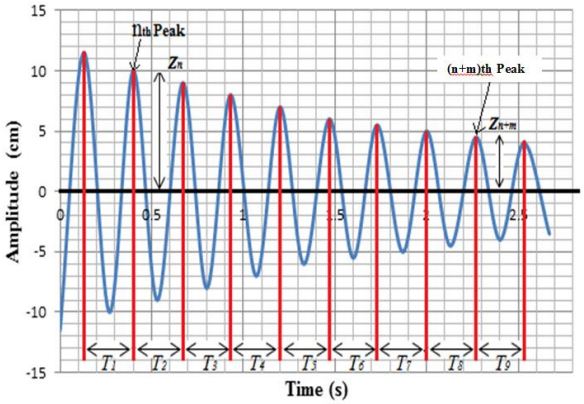

Figure 8 Free damping oscillation at *U*=0

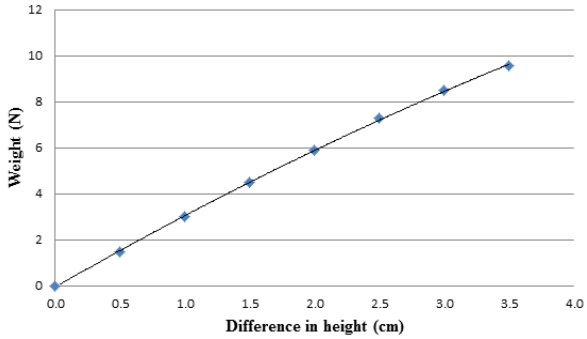

Figure 9 Result of calibration experiment to determine the spring constant

Table 2 Structural parameters

Parameters	k [N/m]	f_n [Hz]	m_e [kg]	δ	Sc
Circular	16.67	3	0.0469	0.00339	1.80
Square	26.04	4.5	0.0326	0.05096	7.24

4.3 Vibration Behaviors

Figure 10 shows the normalized amplitude of cross flow vibration plotted against the reduced velocity *U** for the circular and the square cylinder compared with those reported by T. Nguyen *et al.* [11] and Kawabata *et al*. [12], respectively. The equation $Z_{rms} = Z_A/\sqrt{2}$ obtained from Equation (7) is applied to compare the results.

In spite of the large difference in the experimental conditions and rather rude circumstance and rough measurement of the present experiment, Figure 10(a) shows that the amplitude of KVIV of the circular cylinder is comparable with the wind and water tunnel experiments while the reduced velocity is almost three times higher. In Figure 10 (b), crossflow vibration of the square cylinder is compared with Kawabata *et al*.'s result, which shows KVIV at 7<*U**<9 and galloping at *U**>15. Figure 10(b) seems to show that the galloping of square cylinder is well reproduced by the apparatus of the present work. However, considering the range of *U** in Figure 10(a), there remains a possibility that the vibration at the present work plotted in Figure 10(b) is KVIV but not the galloping.

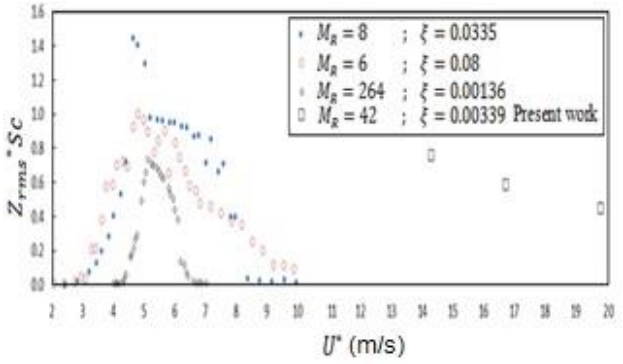

(a)

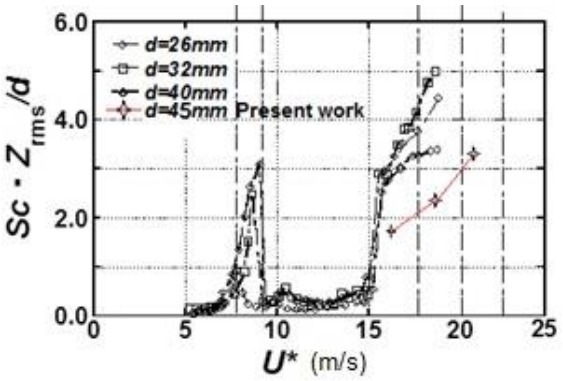

(b)

Figure 10 Results of vibration experiment compared with laboratory experiment by Nguyen *et al*. [11] for circular cylinder and Kawabata *et al.* [12] for square cylinder. (a) Circular cylinder (b) Square cylinder

Figure 11 shows the flutter of the rectangular cylinder coupled with KVIV, which shows the mechanism of the Tacoma Narrows Bridge accident by the simple model.

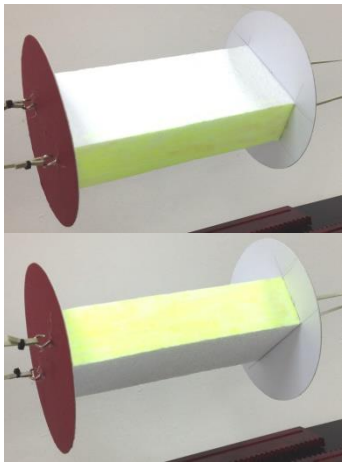

Figure 11 Photograph of torsional flutter of rectangular cylinder

5.0 CONCLUDING REMARKS

We observe FIVs in everyday life and engineering applications, and know that their appearances and behaviors are widely diverging depending on the circumstance where they are occurring. In this article, essential reasoning of the difficulty in FIV problems is reviewed first. Then, one-degree-of-freedom vibration of a cylinder exposed to uniform flow is focused since it is a most typical and of practical engineering importance.

The most common and well-known ones in this category of FIVs are the Karman vortex induced vibration (KVIV), the galloping and the torsional flutter. Hence, in this work, very simple and convenient apparatus to reproduce these three vibrations are designed and fabricated. This apparatus will be effective in fluid mechanics education by demonstrating in a classroom lecture how easily the FIVs can be induced by a simple apparatus, even though their prediction still remains to be an important problem to be solved in practical engineering. The galloping which was not definitely identified by the present apparatus will be reproduced by replacing the fan with a more powerful blower to obtain higher velocity flow.

Acknowledgement

This research was financially supported by the Malaysian Ministry of Education (MOE) under the Fundamental Research Grant Scheme (4F479) and and Research University Grant (08H73) project of Universiti Teknologi Malaysia.

Nomenclature:

c, c_c	Damping factor and critical damping factor [Ns/m]
C_L	Lift coefficient, = $2F_L/\{(\rho U^2 dL\}$ [-]
d	Representative length of cylinder [mm]
F_L	Lift force [N]
F_Z	Fluid force in z-direction [N]
fn	Natural frequency of the system [Hz]
fv	Vortex shedding frequency for oscillating cylinder [Hz]
fv_0	Vortex shedding frequency for the fixed system [Hz]
k	Spring constant [N/m]
L	Span-wise length of cylinder [m]
M_R	Mass ratio [-]
S_C	Scruton number, = $2 M_R\delta$ [-]
U	Free flow velocity [m/s]
U^*	Reduced flow velocity, = $U/(fn.d)$
Z	Displacement of cylinder in crossflow direction [mm]
δ	Logarithmic damping factor [-]
μ	Viscosity of fluid [Pa.s]
ρ	Fluid density [kg/m3]
ζ	Damping ratio, = c/c_c [-]
ω_n	Natural angular frequency, = $2\pi fn$ [1/s]
Subscripts and superscripts	
A	Amplitude
*	Non-dimensional variables
e	Effective values
rms	Root mean square value, representing the amplitude
0	Fixed system

References

[1] Blevins, R. D. 1990. *Flow-Induced Vibration*. Second Edition. Van Nostrand Reinhold. 104-120.
[2] P. W. Bearman. 1984. *Ann. Rev. Fluid Mech.* 16: 195.
[3] Khalak, A. Williamson, C. H. K. 1999. *J. Fluids and Structures.* 13: 813.
[4] Sarpkaya. T. 2004. *J. Fluids and Structures*. 19. 389.
[5] Koide, M. Takahashi, T. Shirakashi. M. 2004. *J. Computational and Applied Mechanics.* 5-2: 297.
[6] Carberry, J. Sheridan, J. Rockwell, D. 2005. *J. Fluid Mech*. 538: 31.
[7] Govarhan, R. N. Williamason, C. H. K. 2006. *J. Fluid Mech*. 561: 147.
[8] Williamson, C. H. K. Govardhan, R. 2007. *J. Wind Eng. and Ind. Aerodynamics*. doi:10.1016/j.jweia.2007.06.019.
[9] Ng, Y. T. Luo, S. C. Chew, Y. T. 2005. *J. Fluids and Structures*. 20: 141.
[10] Klamo, J. T. Leonard, A. Roshko, A. 2006. *J. Fluids and Structures*. 13: 845.
[11] Nguyen, T. Koide, M. Takahashi, T. Shirakashi, M. 2012. *J. Fluids and Structures*. 28: 40.
[12] Kawabata, Y. Takahashi, T. Shirakashi, M. 2009. *JSME. Series B.* 75-754. 1304 (in Japanese).
[13] Morse, T. L. Williamson, C. H. K. *J. Fluid Mechanics.* 634: 5.
[14] Bashford and Thompson Photo. PH Coll. 290.3.